HANbit ACE64 ATM 교환기 시스템의 Twinax 케이블 모델링

정회원 남 상 식*, 박 종 대*

Twinax Cable Modeling for Use in HANbit ACE64 ATM Switching Systems

Sang-sig Nam*, Jong-dae Park* ***Regular Members***

요 약

본 논문은 HANbit ACE64 ATM교환기 시스템의 데이터 경로인 IMI(Inter Module Path)에 사용되는 고속 전송선로인 Twinax 케이블을 two-port lumped Spice-network 모델로 구현하기 위해 lumped 네트워크 요소와 수학적 함수를 사용하여 개발하였다. 사용된 요소들은 저항성분과 주파수의존 전압제어 소스로 구성되어 있고 Hspice 수학적 함수인 FREQ, DELAY, POLY를 사용하여 구현하였다. 구현된 모델을 사용하여 케이블 길이와 종류에 따른 각종 노이즈 분석을 실시하여 그 특성을 비교 분석하였다.

ABSTRACT

In this paper, complete and general two-port lumped Spice-network model is developed for a lossy transmission line. This model is realized as a Spice subcircuit, by means of standard lumped network elements and mathematical functions. It is used as a component in the time-domain simulation of a high-speed data transmission line such as IMI(Inter Module Interface) data path in HANbit ACE 64 ATM switching system. The only required Spice network elements are resistance and frequency-dependent controlled-voltage sources. Such frequency-dependent sources are realized by utilizing the standard Hspice mathematical functions FREQ, DELAY, and POLY

I. Introduction

In digital transmission systems with very high data rates (e.g. 155Mb/s, 622Mb/s) the influence of electrical lead wires on the behavior of the overall circuit can no longer be neglected. Particularly the connection between ASICs on cable assemblies and backplane create a major bottleneck for high-speed signal transmission, and it is clear that their performance determines the integrity of the arriving signal[1,2]. The typical line discontinuities in cable and backplane interconnections cause high transmission loss and signal deterioration, the open structure permits excessive crosstalk and noise.

The HANbit ACE64 is general purpose, high-performance ETRI ATM switching system that can be used in the backbone core as well as the edges of the ATM network. This switching system consists of ATM local switching subsystem(ALS) and ATM central switching subsystem(ACS). The ALS offers interfaces for ATM subscribers (STM-1/4, DS3, DS1E, DS1), frame relay

* 한국전자통신연구원 교환전송기술연구소(parkjd@etri.re.kr)
논문번호 : 99109-0328, 접수일자 : 1999년 3월 28일

subscribers, circuit emulation subscribers, ADSL/HDSL subscribers and N-ISDN. The ALS has also local switching and concentration functions. The ACS is a simple passive switching network for the interconnection between ALSs.

The HANbit ACE64 ATM switching system has a scalable architecture. Thus, it is possible to increase the capacity of the switching system from 32X32 up to 256X256 just by adding ALSs and switching modules in the ACS. The system employs non-blocking self-routing switch module.

All high-speed data signals that connect modules of the HANbit ACE64 switching system operate at 250Mb/s and their connectivity is via metallic cabling using standard 2mm twinax cables and connectors. The high-speed signals are all serial-differential, point-to-point, and are generated by GaAs transceivers. The transceivers are physically located within the Vitesse FX-type GaAs gate arrays. Figure 1 specifies schematic of the physical IMI data path of HANbit ACE64 ATM switching system and describes the connectivity model for the simulation.

In this paper, we studied cabling and packaging issues between modules within the intra- and inter-subsystems. Our objective was to solve the worst case packaging problems, which we identified as those occurring in the scalable system configuration. Thus, complete and general two-port lumped Spice-network model is developed as a lossy transmission line. And it is used as a component in the time-domain simulation of a high-speed data transmission line such as IMI data path in HANbit ACE 64 ATM switching system.

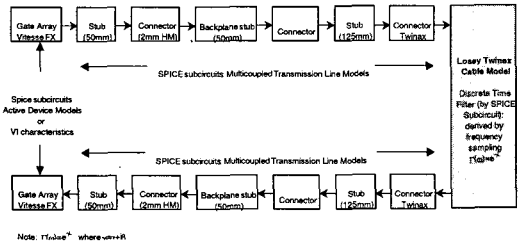

Figure 1. Simulation model of IMI data path in HANbit ACE64 switching system.

Each of the simulation scenarios, described in the table 1 was performed using a field solver to model the physical interconnect. Hspice was also used to calculate the signal integrity for characteristic impedance, crosstalk, ground bounce and voltage noise. The standard components of this schematic include transceivers, stubs, backplane connectors, a stub on a rear I/O transition board, twinax connector pairs, and up to 10 meters of twinax type cables.

Table 1. Simulation Scenarios.

	Connector		Rear I/O Module		Cable Type	
Scen.	Rd. X	STD	Y	N	Gore	A M
1	O			O	O	
2		O		O	O	
3	O		O		O	
4	O		O			O

The twinax cable was modeled as a lossy transmission line to include frequency-dependent skin effect over its length(10m). The lossy transmission line model is an equivalent lumped two-port network that was inserted as a Spice subcircuit into the block labeled Lossy Twinax Cable Model in Figure 1. The derivation of the equivalent two-port network by transmission-line theory[3] is briefly summarized below.

$$v(z, t) = v_F(z,t) + v_R(z,t) \quad (1)$$

$$i(z, t) = i_F(z, t) - i_R(z, t) \quad (2)$$

The general solutions for voltage and current on the line are shown in Eq. 1 and 2 respectively, where the subscripts "F" and "R" denote forward and reverse sinusoidal traveling-wave voltage(v) and current(i) solutions. The voltage traveling wave solutions have the forms given in Eq. 3 and 4 where z denotes distance along the line from one end. Analogous expression follow for $i_F(z,t)$ and $i_R(z,t)$.

$$v_F(z, t) = V_{FM}\, e^{-\alpha z} \cos(\omega t - \beta z) \quad (3)$$

$$v_R(z,t) = V_{RM} e^{+\alpha z} \cos(\omega t + \beta z) \quad (4)$$

Here, the solution of the PDEs yields:

$$\gamma \equiv \alpha + j\beta = \sqrt{(r + j\omega l)(g + j\omega c)} \quad (5)$$

and

$$Z_O = \sqrt{(r + j\omega l)/(g + j\omega c)} \quad (6)$$

where r, l, g and c are the distributed series resistance, series inductance, shunt conductance, and shunt capacitance, respectively, per unit length of the line. γ determines the constants α and β from which follow the attenuation and phase functions in the traveling-wave solutions. The complex impedance Z_O has magnitude and angle. The entire analysis of lossy transmission lines is facilitated by passing from the time domain to the transform domain, which may be interpreted as the generalized phasor, Fourier or Laplace transform domain.

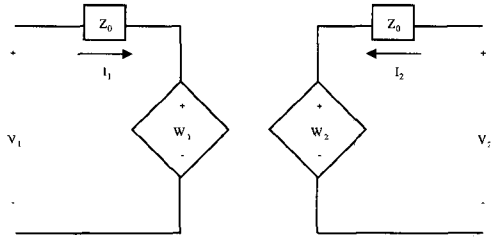

Figure 2. Two-port model of lossy transmission line.

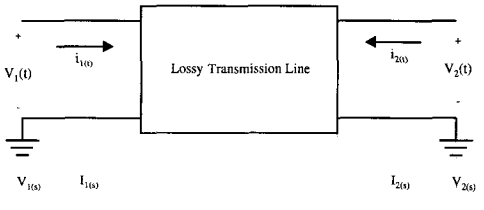

Figure 3. Two-port equivalent network.

Finding the Z parameters now derives the equivalent two port network, shown in figure 2, of a lossy transmission line of length L. Recall the definition of Z parameters[3]:

$$\begin{bmatrix} V_1(s) \\ V_2(s) \end{bmatrix} = \begin{bmatrix} Z_{11}(s) & Z_{12}(s) \\ Z_{21}(s) & Z_{22}(s) \end{bmatrix} \begin{bmatrix} I_1(s) \\ I_2(s) \end{bmatrix} \quad (7)$$

The objective is to relate the terminal voltages $V_1(s)$ and $V_2(s)$ to the terminal currents $I_1(s)$ and $I_2(s)$. This requires the intermediate step of solving the forward and reverse voltage waves. This follows by evaluating the general solution V(z,s) at z=0 and z=L and applying Eq. 1

$$V_1(s) = V(z,s)\big|_{z=0} = V_F(z,s)\big|_{z=0} + V_R(z,s)\big|_{z=0} \quad (8b)$$

$$V_2(s) = V(z,s)\big|_{z=L} = V_F(z,s)\big|_{z=L} + V_R(z,s)\big|_{z=L} \quad (8b)$$

Using the propagation function to relate basic traveling wave solutions at opposite ends of the line:

$$V_F(z,s)\big|_{z=L} = (\Gamma(z,s)\big|_{z=L}) V_F(z,s)\big|_{z=0} \quad (9)$$

and

$$V_R(z,s)\big|_{z=0} = (\Gamma(z,s)\big|_{z=L}) V_R(z,s)\big|_{z=L} \quad (10)$$

where $\Gamma(z,s) \equiv e^{-\gamma z} = e^{-(\alpha + j\beta)z} = e^{-\alpha z} e^{-j\beta z}$.

Thus, the terminal voltages $V_1(s)$ and $V_2(s)$ gives

$$\underbrace{\begin{bmatrix} V_1(s) \\ V_2(s) \end{bmatrix}}_{V} = \underbrace{\begin{bmatrix} 1 & \Gamma \\ \Gamma & 1 \end{bmatrix}}_{B} \underbrace{\begin{bmatrix} V_F(0,s) \\ V_R(L,s) \end{bmatrix}}_{Vw} \quad (11)$$

Likewise, terminal currents $I_1(s)$ and $I_2(s)$ gives

$$\underbrace{\begin{bmatrix} I_1(s) \\ I_2(s) \end{bmatrix}}_{I} = \frac{1}{Z_O} \underbrace{\begin{bmatrix} 1 & -\Gamma \\ -\Gamma & 1 \end{bmatrix}}_{A} \underbrace{\begin{bmatrix} V_F(0,s) \\ V_R(L,s) \end{bmatrix}}_{Vw} \quad (12)$$

Summarizing Eq. 11 and 12:

$$V = BVw \text{ and } I = \frac{1}{Z_0} AV_W$$

where the vectors V, I and V_W and matrices A and B were "defined" in Eq. 11 and 12 by using curly braces. Solving Eq. 12 for VW gives

$$V_W = Z_O A^{-1} I \tag{13}$$

and substituting Eq. 13 into Eq. 11 yields

$$V = Z_O B A^{-1} I \tag{14}$$

where the Z parameter matrix has been identified from Eq. 14 as $Z = Z_O B A^{-1}$. Therefore, the Z parameter matrix gives

$$Z = \begin{bmatrix} \frac{1+\Gamma^2}{1-\Gamma^2} & \frac{2\Gamma}{1-\Gamma^2} \\ \frac{2\Gamma}{1-\Gamma^2} & \frac{1+\Gamma^2}{1-\Gamma^2} \end{bmatrix} \tag{15}$$

It can now be verified that the two port network in figure 2 is equivalent to the lossy transmission line. This can be done most easily by finding the Z parameters of that two port by applying the usual open circuit impedance tests to the network of figure 3.

$$Z_{11}(s) = \frac{V_1(s)}{I_1(s)} \Big|_{I1(s)=0} \tag{16a}$$

$$Z_{12}(s) = \frac{V_1(s)}{I_2(s)} \Big|_{I2(s)=0} \tag{16b}$$

where

$$Z_{21}(s) = Z_{12}(s) \tag{17}$$

always by reciprocity and

$$Z_{22}(s) = Z_{11}(s) \tag{18}$$

by the symmetry of this particular network.

Thus it is only necessary to evaluate Eq. 16 since it is obvious that the reciprocity and symmetry conditions in Eq. 17 and 18 are already satisfied in Eq. 15. Note that $I_2(s)=0$ gives W2=V2 and $I_1(s)=0$ gives $W_1=V_1$ in figure 2. This simplifies the evaluation of Eq. 16, which the reader may verify and reduce to the appropriate entries in Eq. 15.

Ⅱ. Realization of Equivalent Network by Spice

Realization of the Spice subcircuit for equivalent lumped two port network in figure 2 is accomplished as follows. The network in figure 2 is mirrored directly by the Spice netlist, which defines nodes interconnected by the resisted elements $R=Z_0$ and the controlled voltage sources W_1 and W_2.

Following this preliminary topological definition of the Spice network, the problem reduces to the realization of the equations,

$$W_1(\omega) = \Gamma(\omega) \bullet (2V_2 - W_2) \tag{19}$$

and

$$W_2(\omega) = \Gamma(\omega) \bullet (2V_1 - W_1) \tag{20}$$

which control the voltage sources W_1 and W_2. This is done by using the Hspice mathematical functions POLY, DELAY and FREQ, which will be explained with the aid of the figure 4. Figure 4 consists of a copy the network in figure 2 with the addition of flow graphs containing the following Hspice elements: POLY, DELAY, FREQ, auxiliary controlled voltage sources, and auxiliary nodes. The elements are all shown below the horizontal ground line of the original network.

It should be noted that the original network, including the defining equations of W_1 and W_2, is completely symmetric. It is, therefore, adequate to explain the computation of W_1 from V_1 and W_1; the computation of W_2 from V_2 and W_2 follows by symmetry. Also note that all auxiliary controlled voltage sources and auxiliary nodes in the flow graphs are introduced only to conform to Spice requirements for signal voltage interfaces. They have no mathematical function.

The first step is to compute the linear combination $2V_1-W_1$ by the POLY function, which is actually a first order approximation by a polynomial in V_1 and W_1. It only remains to realize the propagation function $\Gamma(\omega)$ in cascade

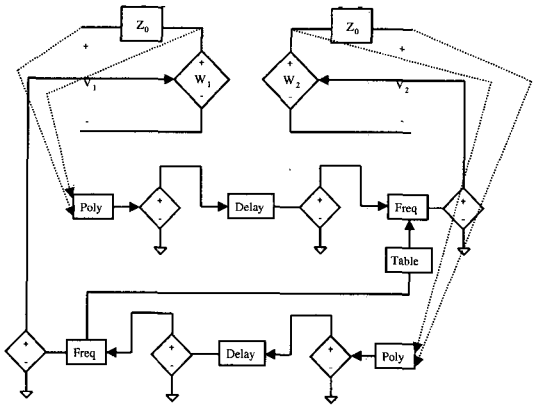

Figure 4. Spice realization Lossy transmission line model.

with $2V_1$-W_1, by means of the Hspice DELAY and FREQ functions. The realization of $\Gamma(\omega)$ is separated into a cascade of two parts: the magnitude function $e^{\alpha z} \mid_{z=L} = e^{\alpha L}$ and the phase function $e^{-j\beta z} \mid_{z=L} = e^{-j\beta L}$. The method used to realize the magnitude function is equivalent to a finite impulse response(FIR) discrete-time filter with linear phase. The magnitude characteristic is input to the Hspice discrete time filter (FREQ) function by means of a previously computed lookup table of values at discrete points. This amounts to the "frequency sampling" method of FIR discrete-time filter design. The phase function for the lossy line is assumed to be equivalent to a constant delay (i.e. a linear phase). Since the phase function is determined by β from Eq. 5, this assumption amounts to ignoring the dependence of on the losses r and/or g in Eq. 5. This is a reasonable assumption because β is affected significantly by loss only at high loss levels. The specific magnitude function used for lossy cable is based on the assumption that cable attenuation is dominated by skin effect. In this case, α is proportional to $\sqrt{\omega}$, which is to say that r in eq.5. is a function of ω. Thus a table is built for input to the Hspice **FREQ** function based on α. The scale factor for the table is determined from the cable manufactuers data, which gives the actual value of attenuation α at a specific frequency ω.

The Hspice mechanism that supplies the phase function is the **DELAY** element. Thus the resulting frequency dependent controlled voltage source and the **DELAY** elements are cascaded between each of the previously mentioned auxiliary nodes and the nodes that control their corresponding voltage sources W_1 and W_2. This produces the overall propagation function for Eq. 19 and 20. This two-port lumped network model for the lossy transmission line is quite unique for the Spice environment. It includes the frequency dependent properties of the line due to skin effect and cross-coupling properties that accurately simulate multiple reflections within the overall system.

Ⅲ. External HS Data Path Simulation Results

The simulated data path for external high speed signals was performed according to figure 1, and the simulation results for all of the scenarios, case 1 through 4, described in the table 1 are shown in the following figures. In all cases the driver waveform is a pulse with minimum and maximum levels of 0 volts and 1 volt, respectively. The pulse rise time is on the order of 0.5ns. The standard tests included here are the reflection test, at the far end or output signal, and the near and far end crosstalk tests. These are shown in the upper and lower frames of each figure.

The reflection test is essentially a measure of the effect of accumulated discontinuities in the signal propagation path; ideally such effect will be negligible. The crosstalk test is a measure of the relative degree of cross coupling due to mutual capacitance and mutual inductance. The criteria of acceptability for the reflection and crosstalk tests defined as follows. For the reflection test the accumulated reflections after a pulse transition (i.e., a switching transient) must not be large enough to violate the logical threshold with respect to the newly established signal level. Likewise for the crosstalk test the

signal that is cross-coupled into the victim line must not be large enough to violate threshold with respect to the pre-existing signal level.

A quick examination of the case figure verifies that the reflection and crosstalk test indicate acceptable performance in all cases. In fact, the performance is excellent; The reflection effects are negligible and the crosstalk level is extremely small (20mV to either side of the average or reference base line). The crosstalk level does not come close to violating logical thresholds.

The most significant variation among the various cases is in the signal level at the far-end or output signal. Clearly this can be attributed tothe changes in attenuation of the lossy twinax cable. This is caused by the differences in manufacturer as seen in the table of scenarios given in the previous section.

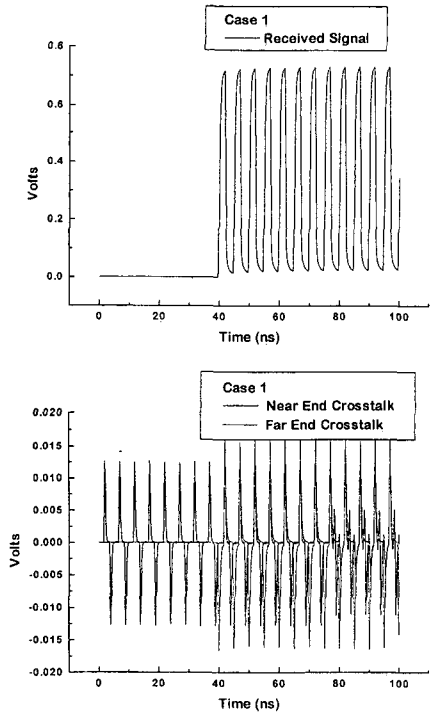

Figure 5. Reflection and Crosstalk Waveforms Lossy Cable HS Signal(Case 1)

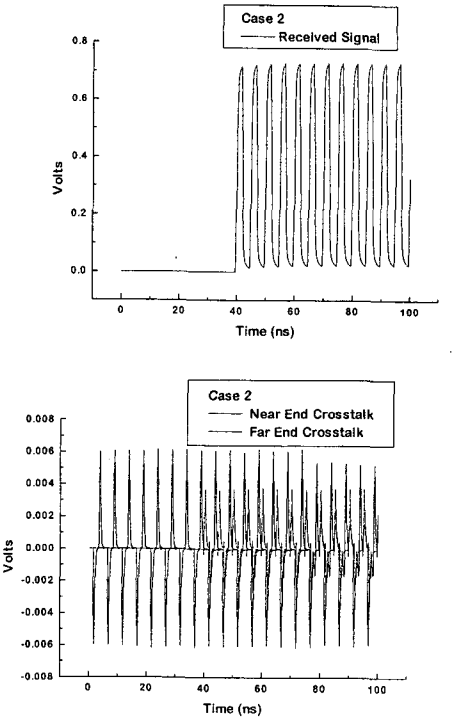

Figure 6. Reflection and Crosstalk Waveform Lossy Cable HS Signal (Case 2)

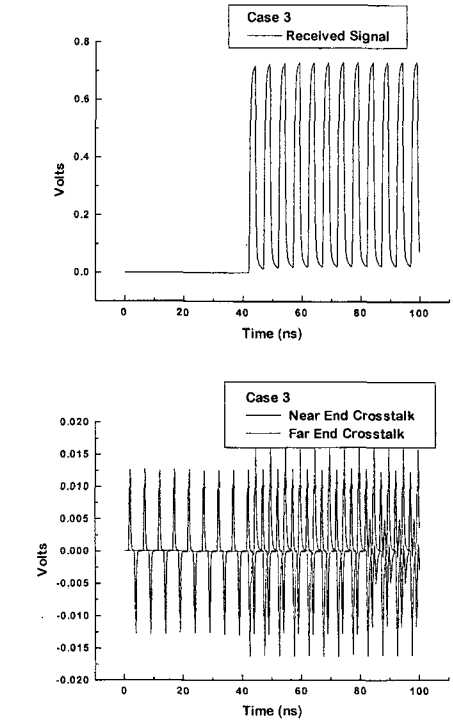

Figure 7. Reflection and Crosstalk Waveform Lossy Cable HS Signal (Case 3)

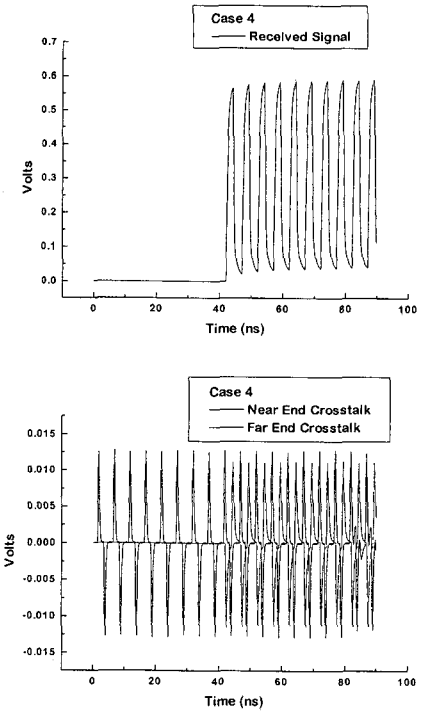

Figure 8. Reflection and Crosstalk Waveform Lossy Cable HS Signal (Case 4)

Ⅳ. Conclusions

We have developed a complete and general two-port lumped Spice-network twinax cable model for a lossy transmission line. This model is realized as a Spice subcircuit by means of standard lumped network elements supported by mathematical functions. The subcircuit is used in a time-domain simulation of the high-speed data path of HANbit ACE64 ATM switching system. The simulation results are showed that the crosstalk tests indicate acceptable performance in all cases. This techniques developed as part of this paper will be applied to several areas of signal integrity analysis.

참 고 문 헌

[1] A. J. Groudis and C. S. Chang, Coupled Lossy Transmission Line Characterization and Simulation, *IBM J. RES. DEVELOP*, Vol. 25, No.1, pp. 25-41, Jan. 1981.

[2] A. C. Cangellaris and J. L. Prince, Modeling and Simulation for Mixed-Signal Package Design, *Advances in ElectronicPackaging 97 Conf.*, EEP-Vol.19-1, pp.497-504, Jan.15-19, Hawaii, 1997.

[3] Younkang Chin, *Microwave Engineering*, Chungmoongak, Seoul, 1993.

남 상 식(Sang-sig Nam) 정회원
통신학회논문지 제22권 제1호 참조.
현재 : 한국전자통신연구원 교환전송기술연구소
ATM기술연구부 책임연구원
<주관심분야> ATM Technology, Signal Integrity

박 종 대(Jong-dae Park) 정회원
통신학회논문지 제 22권 제9호 참조.
현재 : 한국전자통신연구원 교환전송기술연구소
ATM기술연구부 선임연구원
<주관심분야> 집적회로 설계, Signal Integrity